Performance of Distributed Optical Fiber Sensors (DOFS) and Digital Image Correlation (DIC) in the monitoring of RC structures

IOP Conf. Series: Materials Science and Engineering **615** (2019) 012101 doi:10.1088/1757-899X/615/1/012101

Performance of Distributed Optical Fiber Sensors (DOFS) and Digital Image Correlation (DIC) in the monitoring of RC structures

M F Bado[1,2*], G Kaklauskas[1] and J R Casas[2]

[1] Department of Reinforced Concrete Structures and Geotechnics, Vilnius Gediminas Technical University (VGTU), Saulėtekio al. 11, Vilnius 10221, Lituania
[2] Department of Civil and Environmental Engineering, Technical University of Catalonia (UPC), cJordi Girona 1-3, 08034 Barcelona, Spain

[*]Corresponding Author E-mail: mattia-francesco.bado@vgtu.lt

Abstract. Distributed Optical Fiber Sensors (DOFS) are strain measuring tools whose potential related to the civil engineering field has been discovered in the latest years only. A unique utility lies in the possibility of bonding these extremely thin sensors to steel reinforcement bars which will later be embedded in concrete elements (RC) in order to monitor its mechanical strains. The present paper presents the results of an experimental campaign that saw the tensing of two RC tensile members (ties) with DOFS-instrumented steel rebars providing strain readings every 7.5mm. Their cracking behavior allows to gain insight on the steel rebar's strain profile when surrounded by cracking concrete. The described results are novel as measurements that are accurate, completely distributed, experimentally extracted, both before and after concrete cracking, have been impossible up until now. The internal strain measurements are additionally integrated with an external Digital Image Correlation (DIC) monitoring which provides data on the displacements and strains of the members' surfaces. The present research represents the beginning of an in-depth experimental campaign aimed at providing reinforcement strain data for multiple loaded RC ties encompassing different geometrical features (concrete cover, reinforcement ratio, bar diameter).

1. Introduction

The most pivotal point behind the behavior of RC structures is the concrete-steel reinforcement bars (rebar) interaction. Modern research decided to set aside the commonly assumed theory of perfect interaction between the two materials or simplified constant bond relations [1] in favor of a *stress-transfer approach*. The latter suggests a continuous interaction between the two materials in the form of a force transfer along their contact surface (bond stress τ_b) which varies according to the *slip* (wherever the absolute displacements of concrete and steel are dissimilar). Despite this phenomenon being extensively investigated both analytically and experimentally over the years [2, 3] an overall satisfactory prediction of the bond-slip behaviour has not been achieved and there are large discrepancies among existing bond-slip models [4, 5]. A methodology of studying such relationship consists in extracting the bond slip behaviour of reinforcement by studying the profiles of the strains suffered by the reinforcement bars embedded into the concrete along the member [6].

Consequently, an accurate measurement of the variation of ε_s along the rebar is the key to an equivalently accurate bond stress profile depiction at a specific instance. Despite in the past numerous technique and sensing tools were used with the goal of measuring such profiles (milling a groove in a rebar's core and gluing strain gauges or instrumenting with FBG sensors) [1, 7, 8] , none of them could boast the advantages of DOFS. These are very thin glass wires (125 μm of diameter, similar to a hair's thickness as in figure 1a) able to accurately measure strains (1με), temperature and vibration in 2 or even 3 dimension and in a completely-distributed manner (every millimeter) with flexible spatial resolution and of the desired frequency.

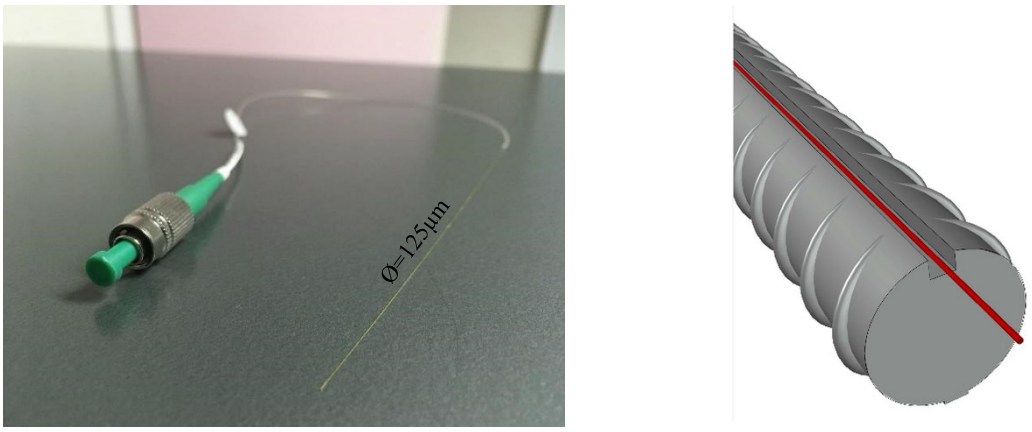

(a) (b)

Figure 1. (a) DOFS fiber (b) Representation of a DOFS inserted in a groove milled in a steel rebar.

The instrumenting of RC ties with DOFS has been developed in few experimental tests before [9, 10, 11]. The experimental campaign designed by the authors follows the technique that some authors [12, 9] designed in order to protect the fiber from the friction with cracking concrete. This consisting in incising a groove on the side of the rebar (along the longitudinal ridge) and positioning the DOFS inside it (as visible in figure 1b) ensuring the bond with an adhesive.

Finally, the results showed in the present publication are integrated with the external monitoring method of Digital Image Correlation (DIC). The latter is a cheap non-contact optical technique for measuring strain and displacement. DIC works by comparing digital photographs of a component or test piece at different stages of deformation. By tracking blocks of pixels, the system can measure surface displacement and build up full field 2D and 3D deformation vector fields and strain maps [13]. This was developed with the help of a software called GOM Correlate [14].

2. RC specimens and test setup

The present paper covers the experimental results of three tested RC tensile members. Their geometrical and material mechanics features are listed in table 1 below. These elements are part of a large experimental campaign developed in the UPC´s Structure Technology Laboratory that sees the tensing of multiple RC members with different geometrical characteristics such as rebar diameter $Ø_s$, cover size, reinforcement ratio ρ_s, prismatic length L and cracking features (some prism are designed to crack while others are designed not to).

Table 1. Geometrical and material features of the tested RC tie members.

Member n.	Member code	Prism size/s (cm)	Prism length/s L (cm)	Rebar diameter $Ø_s$ (mm)	f_c (MPa)	E_c (MPa)	f_{ct} (MPa)	f_y (MPa)
1	10x10_D12.01	10x10	60	12	37.65	34939	2.96	537.17
2	10x10_D12.02	10x10	14,16,18	12	40.94	31198	3.17	537.17
3	10x10_D16.02	10x10	60	16	40.94	31198	3.17	650.81

Graphical representation of the RC ties

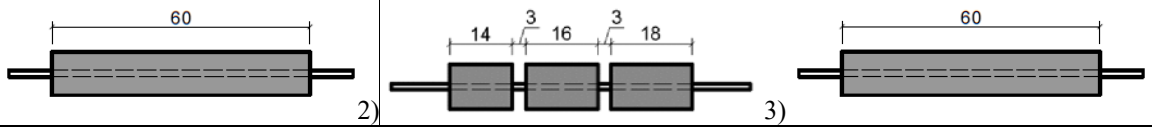

This, as a combined effort from VGTU and UPC universities finalized to studying the steel rebars' strain profiles when embedded inside concrete and subjected to different levels of tensile strain. As mentioned above the information is crucial to the development of new RC bond stress and bond-slip laws which, differently than what was developed before, are grounded on accurate, completely distributedly and non-intrusively gathered strain data.

The concrete mix consisted of 182 kg/m^3 of water, 363 kg/m^3 of Portland cement, 968 kg/m^3 of fine aggregate and 968 kg/m^3 of coarse aggregate with an adding of super-plasticizer. The members were subjected to monotonic tensile stress at a constant loading speed of 0.1mm/min by means of an INSTRON hydraulic actuator (figure 2) until the DOFS reported strains equals or above the steel yielding strain f_{ys}. The strains inside the members were monitored through 1.22m long DOF sensors (bonded to the rebars) by means of an OBR ODiSI-A manufactured by LUNA Technologies [15]. The spatial resolutions selected for the current tests were of 7.5-10 mm with measurements every 3.2-5 seconds. Meanwhile, the external displacements of the RC ties were instead measured through DIC technology. In particular, a 24 MPx camera was taking picture of the deforming member at constant intervals of 5 seconds. Later the taken pictures were compared and the displacement calculated by means of GOM.

Figure 2. Experimental setup with photo camera set to take pictures at regular intervals.

3. DOFS strain readings post-processing

Once the DOFS measurements were completed and all the strain data collected, the first step in its post-processing consists in studying and compensating for its anomalistic readings (SRAs) which present themselves as abnormally high strain peaks [16]. These ones might distort the strain profiles provided by the DOFS and OBR as studied in the previous research by the author´s research team. In particular,

Harmful Anomalies (HF-SRAs) are followed by additional anomalies for all the remaining duration of the test while others that (extremely disruptive for the test) while Harmless anomalies (HL-SRAs), despite preventing the correct reading of the strains at a specific instance, still allow it later. Once determined which SRAs are harmless and which harmful it is possible to proceed to their elimination. Starting from the latter being the nature of this anomaly punctual in nature, the trend of every sensing section of the DOFS has to be studied. Let us take as example figure 3a, reporting the strain measurement taken by a 1.22m long fiber bonded to the Ø16 bar of member 10x10_D16.02. In particular, the dashed black line represents the original data as measured by the OBR in DOFS coordinate 0.69 m along the whole duration of the test.

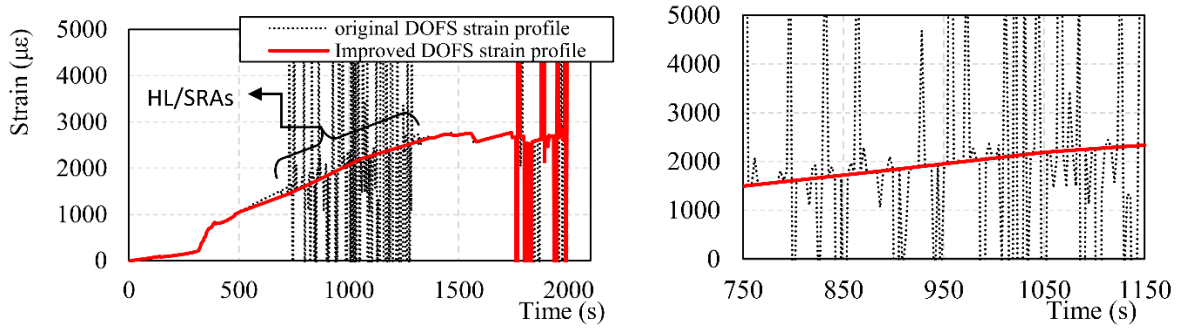

Figure 3. (a) DOFS strain readings along the test of DOFS section 0.69m (b) zoom of the graph on the left to highlight the quality of the fit between original and improved profiles.

Hardly any reliable measurements can be extracted between more or less 750s and 1300s as SRAs are predominant. The Spectral Shift Quality (SSQ) displays a calculated merit function to assess the quality of the measurement (as a function of the frequency shift of the light reflected from the fiber) between the baseline and the measured data [15]. It is here used as a tool to assess the reliability of the DOFS measured data. If to interpolate only the points with highest SSQ values a trend-line can be drawn (in red in figure 3) which closely reproduces the DOFS measurements but this time HL-SRA-free. For the present section the best fit can be achieved through the removal, and consequent recalculation through point interpolation, of any measurement with SSQ lower than 0.2. Figure 3b shows how the trend-line interpolates all the most reliable points to form the most realistic SRA-free DOFS strain profile. With such correction a strain profile encompassing every section at a specific instance of the experimental test won´t show anymore SRAs in the 0.69 m section (figure 4).

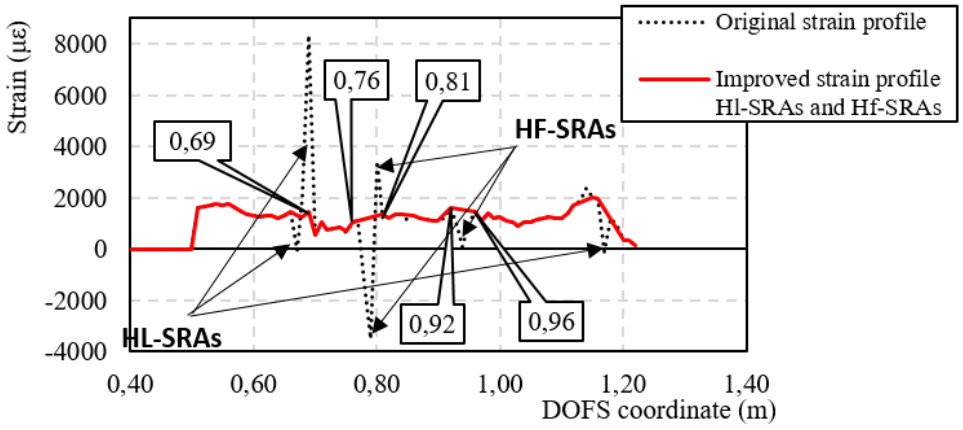

Figure 4. DOFS strain profile at 729 s and 55.16 kN with and without anomalistic corrections.

In order to remove the HF-SRAs, the strain profile graph encompassing all DOFS coordinates must be considered as in figure 4. DOFS strain profile at 729 s and 55.16 kN with and without anomalistic corrections (at instance 729 seconds and at tensile load of 55.16 kN). Once again the SSQ limit should be set and the DOFS strain readings with correspondent SSQ values lower than the set value, eliminated and substituted by an interpolated value. The DOFS profiles displayed in the following, whenever possible, have been cleaned up from SRAs of both kinds.

4. DOFS and DIC strain analysis for the study case members

In the following the steel rebars' strain profiles inside the concrete prisms (members 10x10_D12.01 and 10x10_D16.02) will be displayed in the context of the two main stages that characterizes a RC tie member behavior. These are the Elastic stage and the Cracking stage. DIC will here be assisting in pointing out the moment and the sections where the cracks appear. Additionally, member 10x10_D12.02 displays the evolution of strains in three short RC elements having their section smaller than two transfer lengths, thus making impossible the cracking of these elements with strains simply increasing along the test.

4.1. Cracking members

Figure 5 represents the strain profiles of members 10x10_D12.01 and 10x10_D16.02 as measured by their respective fibers at an applied load of 5.0 kN (when no cracks have appeared yet). It is worth noting that the strains reported between DOFS coordinates 0.00 m and 0.48 m are equal to zero as the fiber isn't bonded to any surface in this segment and therefore measures nothing all test long. Hereon after this section of the DOFS' measurements won't be represented anymore. Just before the DOFS is embedded in the RC prism (0.48m-0.53m) it is shortly glued to the rebar, hence a rise in strains equal to equation (1), corresponding to 126με for the larger diameter bar and 221με for the smaller one.

$$\varepsilon_s = \frac{N}{E_s A_s} \tag{1}$$

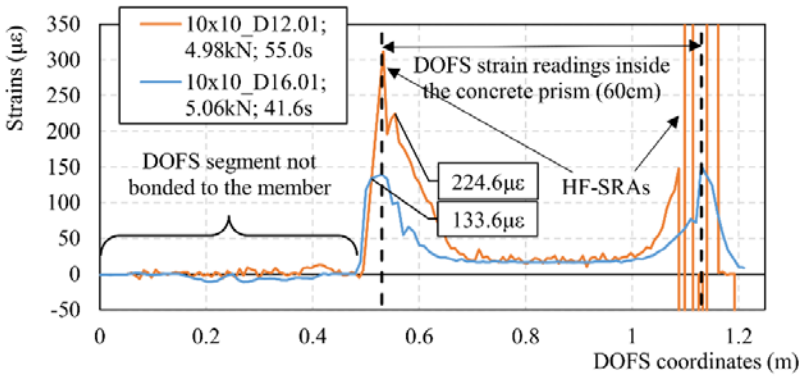

Figure 5. DOFS strain measurements of members 10x10_D12.01 and 10x10_D16.02 loaded with a 5.00 kN tensile force.

Unfortunately, in the case of member 10x10_D12.01, this instance coincides with an HF-SRAs on both extremities of the concrete prism which makes it hard to extract accurate readings. Yet the strain values of DOFS coordinates in the proximity indicate result very similar to the expected ones. The rebars' strains immediately start decreasing as the first section of the rebar's is embedded in the concrete prism (0.54m) as the mechanism of stress transfer between steel and concrete is triggered reaching the lowest value around the DOFS coordinate 0.70 m where a state of strain compatibility is reached resulting in a similar ε_s and ε_c.

As the tensing load increases along the test, the strains of both steel and concrete increase, including the compatibility zone. This, up until the point where the maximal tensile strength of concrete is reached

in any transversal section of the member and, unable to carry any more stresses, the concrete cracks. The cracking stage is now underway. Figure 6 represents the first instance where this phenomenon was recorded by the DOFS. In particular, for member 10x10_D12.01 this occurred after 110 seconds at a tensile load of 9.0n kN while this occurs for member 10x10_D16.02 at a later stage due to its larger bar diameter (144 seconds, 16.2 kN). As expected the strains peak in the cracked section as the concrete cannot help the steel rebar carrying any stresses. Consequently, in the case of completely developed cracks, the latter is singularly resisting the entire tensile force in the cracked section.

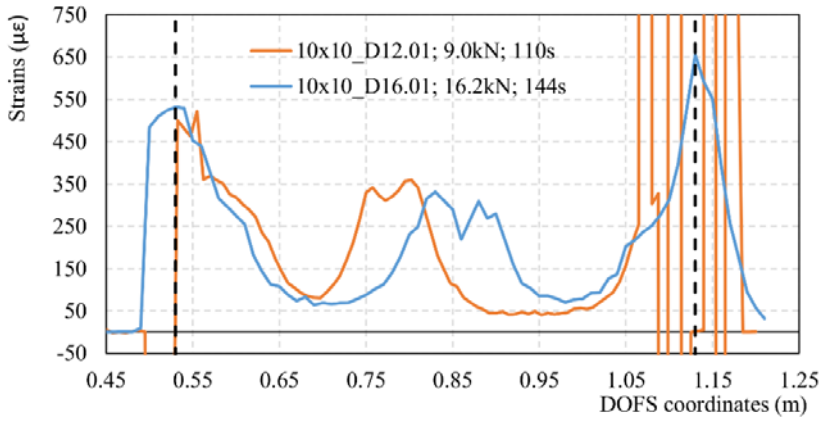

Figure 6. DOFS strain measurements of members 10x10_D12.01 and 10x10_D16.02 in the first instance that a crack appears.

Figure 7 reports the output of a DIC major strains analysis of the two members. The first six show the evolution of the crack in member 10x10_D16.01 at different time stages whilst the last one shows a late deformation time stage of member 10x10_D12.01 that already displays multiple cracks. If to verify the correlation between the location of the crack and the strain peaks of figure 6, it is noticeable how the two match perfectly, confirming that a strain peak marks indeed the member section where a crack will form. Between the appearance of the strain peaks (crack start internally) and its appearance on the surface of the member a certain amount of time passes as visible from the different time stamp in the two figures. This time difference and the simultaneous evolution of strains on the rebar and on the surface will be the subject of further publication by the authors.

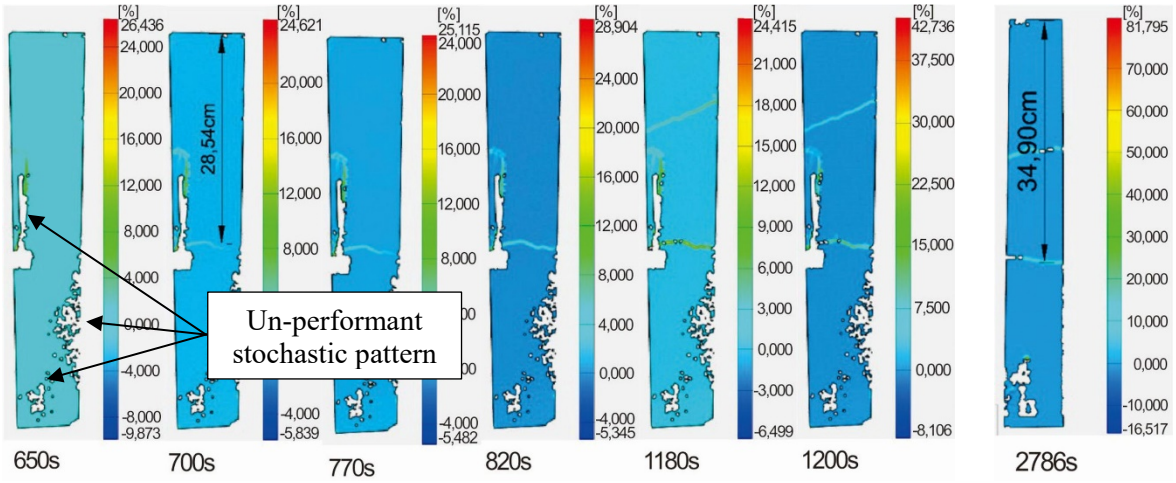

Figure 7. DIC pictures processed through GOM Correlate to extract Major Strains (a) for member 10x10_D16.01 and (b) for member 10x10_D12.01.

4.2. Non-cracking member

If to consider concrete RC members whose total length is smaller than s_{rm} (the average crack spacing for a member as assessed by the Eurocode 2), it would be possible to see how an increase in stresses does not lead to any crack formation. Figure 8 plots the strain evolution inside three RC members jointly called 10x10_D12.01 during five load stages ranging from 2.59kN to 48.85kN. Please keep in mind that this member was not designed as a simulation of a possible RC tie in real life but rather a convenient setup to test multiple smaller RC ties with one single DOFS. As expected no cracks form even at the later stages while the strains increase proportionally to the applied load. It is worth mentioning that some HF-SRAs are present between concrete Block 1 and 2 and at the edge of the Block 3 in proximity to where the mechanical clamp grips the bar in order to tense it. As mentioned earlier, these profiles are ideal for constitutive modelling and as such this will be the topic of upcoming publications from the authors.

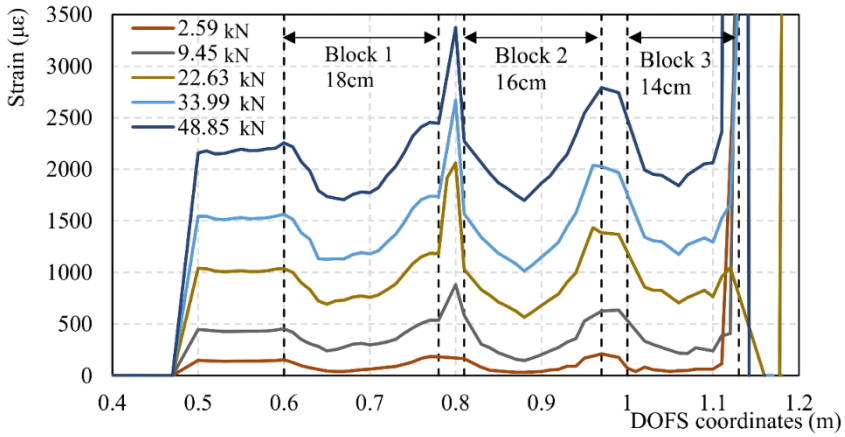

Figure 8. DOFS strain measurements of members 10x10_D12.02 for increasing loading value.

5. Conclusions

This paper's objective was to demonstrate the ability and performance of the combined techniques of DOFS and DIC for strain monitoring both internal and external of RC ties. In particular, the optical fibers were bonded to the rebars of three RC ties having different diameter (Ø12 and Ø16) and different concrete prisms length in which they are embedded. In addition, some concrete prisms were designed to be short enough to prevent the rise of any crack inside them at any load level.

The monitoring of strains in the RC ties, when subjected to monotonic tensile force, was overall successful despite the rise of some SRAs. While the HL-SRAs were removed with an SSQ-based method, the only way of compensating for the HF-SRAs was to remove the reading from the DOFS section under consideration and linearly interpolate the measurements before and after.

With the help of such post-processing techniques the authors were able to extract accurate strain profiles both during the pre-cracking and cracking stage of the RC tie tensile behavior. As expected the first are mainly dominated by an area of compatibility between steel and concrete strain which is only broken on the edges of the members. Later, as the tensile load is increased, the DOFS successfully recorded a peaking of strains where the compatibility of strains is lost due to the rise of a crack inside concrete.

Externally wise, the DIC confirms the location of the rebar's strain peaks to be connected with the appearance of cracks on the surface despite there being a shift between the time of recording of the peaks on the rebar and the cracks on the external surface of the members.

Finally, very clear strain profiles were extracted in the short span members. In this case the evolution of strains for multiple load levels was reported as a testament of the performance of DOFS even at higher

strain levels. A drastic increase in applied load shifts the curves upwards providing an excellent grounding for constitutive modelling as will be demonstrated by the authors in future publications.

In conclusion, the combined use of DOFS and DIC provides the researcher of an excellent monitoring system that, through a constant interaction and check between external and internal strain readings, is provided with a complete picture of the strain distribution inside the members.

Acknowledgment
The first and second authors gratefully acknowledge the financial support provided by the European Social Fund according to the activity 'Improvement of researchers' qualification by implementing world-class R&D projects' of Measure No. 09.3.3-LMT-K-712 Project No.09.3.3-LMT-K-712-01-0145).

References

[1] Kaklauskas G, Sokolov A, Ramanauskas R and Jakubovskis R 2019 *Reinforcement Strains in Reinforced Concrete Tensile Members Recorded by Strain Gauges and FBG Sensors : Experimental and Numerical Analysis* p 1–13
[2] Diab A M, Elyamany H E, Hussein M A andAl Ashy H M 2014 Bond behavior and assessment of design ultimate bond stress of normal and high strength concrete *Alexandria Engineering J.* **53**(2) 355–371
[3] Wu Y-F and Zhao X-M 2012 Unified bond stress–slip model for reinforced concrete *J. of Structural Engineering* **139**(11) 1951–1962
[4] American Concrete Institute (ACI) 1995 *Building code requirements for reinforced concrete* in ACI Committee 318
[5] CEB-FIP 1993 *CEB-FIP model code 1990*
[6] Ruiz M F, Muttoni A and Gambarova P G Analytical modeling of the pre – and post – yield behavior of bond in reinforced concrete *J. of Structural Engineering* **133**(10) 1–27
[7] Kankam C K 1997 Relationship of Bond Stress, Steel Stress, and Slip in Reinforced Concrete *J. of Structural Engineering* **123**(1) 79–85
[8] Houde J 1974 *Study of Force-Displacement Relationships for the Finite-Element Analysis of Reinforced Concrete* (Canada: McGill University, Montreal, Quebec)
[9] Michou A, Hilaire A, Benboudjema F, Nahas G, Wyniecki P and Berthaud Y 2015 Reinforcement-concrete bond behavior: Experimentation in drying conditions and meso-scale modeling *Engineering Structures* **101** 570–582
[10] Zych M, Bednarski L, Howiacki T and Sien R 2018 *Strain and crack analysis within concrete members using distributed fibre optic sensors*
[11] Davis M, Hoult N A and Scott A 2016 Distributed strain sensing to determine the impact of corrosion on bond performance in reinforced concrete *Construction and Building Materials* **114** 481–491
[12] Quiertant M *et al.* 2012 Deformation Monitoring of Reinforcement Bars with a Distributed Fiber Optic Sensor for the SHM of Reinforced Concrete Structures *NDE 2012* pp 1063–1073
[13] McCormick N and Lord J 2010 Digital image correlation *Mater. Today* **13**(12) 52–54
[14] GOM 2016 GOM *Correlate Professional* vol 49(0) p 1–127
[15] LUNA ODiSI-A Distributed, Optical Interrogator, Sensor Guide, Users
[16] Bado M F, Casas J R and Barrias A 2018 Performance of Rayleigh-Based Distributed Optical Fiber Sensors Bonded to Reinforcing Bars in Bending *Sensors, no. Special Issue Bridge Structural Health Monitoring and Damage Identification* p 23